PAPER Special Section on Recent Progress in Electromagnetic Theory and Its Application

Second-Order Perturbative Analysis with Approximated Integration for Propagation Mode in Two-Dimensional Two-Slab Waveguides

Naofumi KITSUNEZAKI[†a)], ***Member***

SUMMARY We calculated propagation constants of supermodes for two-dimensional two-slab waveguides, with small core gap, using second-order perturbation expansion from gapless slab waveguide system, and compared our results with the existing works. In the perturbation calculation, we used trapezoidal method to calculate the integral over the transverse direction in space and obtained second-order expansion of (core gap)/(core width) for propagation constants. Our result can explain the qualitative relationship between the propagation constants and the gap distance in the neighbor of (core gap)/(core width) being zero.

key words: *propagation constants of supermodes, second-order perturbation, two-slab waveguides, Maxwell's equation, Schrödinger's equation*

1. Introduction

When monochromatic light enters into one waveguide of two parallel waveguides systems having the same core width, it is well known that the light propagates in a longitudinal direction while periodically changing waveguides one after the other. Such a behavior has been analyzed based on various analytical methods, including the coupled mode equation or the coupled power equation [1]–[3], matrix method [4], and various numerical methods [5]–[7].

When the distance between the cores of respective waveguides, which is referred to as core gap in the following text, is much larger than the core width, and when light propagates in one of the cores, the amplitude of the light out of the core falls exponentially and that in the adjacent core can be neglected. Based on this fact, coupling mode theory has been derived from the Maxwell's equations using an electromagnetic field in a waveguide array superposed by eigenmodes of the respective waveguides with the slowly varying envelope approximation. An interaction between one eigenmode and the adjacent waveguide has been perturbatively introduced [2]. Electromagnetic field in transverse direction is a solution of the Schrödinger equation, which is derived from the Maxwell's equation. In the field of optics, the Schrödinger equation is often referred to as the Helmholtz's equation.

On the other hand, when the core gap is much smaller than the core width so that the amplitude of the propagating light in the adjacent core cannot be neglected, the basis of coupling mode theory is invalid. Instead of using propagating modes for respective waveguides, even and odd mode analysis was proposed by Suematsu and Kishino [8], which was later referred to as supermode analysis [9].

The Schrödinger equation is well known as a fundamental equation in quantum mechanics, and perturbation analysis is used as a major approximation method to solve the Schrödinger equation, when slight deformation of potential makes the quantum system exactly solvable [10], [11]. In our optical system, the index distribution, which essentially corresponds to potential in quantum system, for two cores with small gap becomes one gap-less core with twice width when the index distribution is slightly deformed. As the optical model for one core slab waveguide can be exactly and easily solved, that for the two-slab waveguides with small gap is appropriate for perturbative analysis.

In this study, we calculated the propagation constants of supermodes for two-dimensional two-slab waveguides based on second-order perturbation from gap-less system, and compared the result with analytic and numerical results reported in the existing works [5]–[7]. Because our analysis is based on a gap-less single waveguide, it would be still easy to analyze an optical behavior in a waveguide array by using perturbation analysis if the number of waveguide in the array is increased. We restricted our discussion regarding electromagnetic field in the TE mode according to these works.

2. Model

Figure 1 shows the spatial configuration of our optical model where two symmetric slab waveguides are configured in parallel. The two cores have the same index n_1 and the same core width w, and clads with index n_2, where n_1 and n_2 are constant, and $n_1 > n_2$. The core width w, core gap d, and indices n_1 and n_2 are chosen so that there are only one symmetric and one anti-symmetric propagation modes. Index distribution $n(x)$ is set as:

$$n(x) = \begin{cases} n_2, & |x| < \frac{d}{2}, \\ n_1, & \frac{d}{2} < |x| < \frac{d}{2} + w, \\ n_2, & \frac{d}{2} + w < |x|, \end{cases} \tag{1}$$

which is constant, except for $x = \pm\frac{d}{2}$ and $x = \pm(\frac{d}{2} + w)$, as shown in Fig. 1(a). The index distribution is constant in the

Manuscript received April 23, 2013.
Manuscript revised August 4, 2013.
[†]The author is with Aoyama Gakuin University, Sagamihara-shi, 252-5258 Japan.
a) E-mail: kitsunezaki@it.aoyama.ac.jp
DOI: 10.1587/transele.E97.C.11

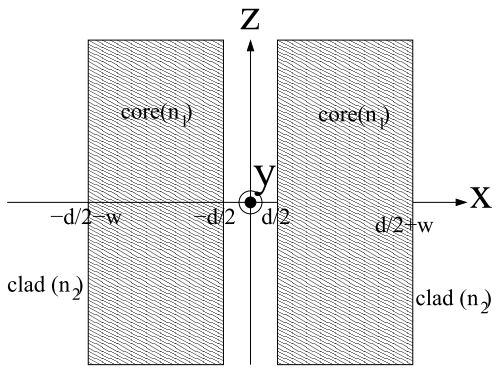

(a) Optical system configuration

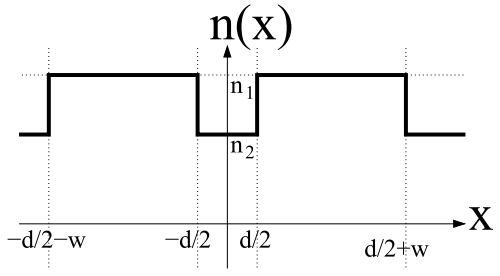

(b) index distribution on z = const. line

Fig. 1 Optical system.

y and z direction. The z direction is defined by the direction to propagate light. The angular frequency of the monochromatic light is ω.

As index distribution has no y-directional variation, electromagnetic fields do not depend on y. For electric field $\vec{E}(t,x,z)$ and magnetic field $\vec{H}(t,x,z)$, the time variable t can be separated from spatial variables to $\vec{E}(t,x,z) = e^{i\omega t}\vec{e}(x,z)$ and $\vec{H}(t,x,z) = e^{i\omega t}\vec{h}(x,z)$, because we are interested in monochromatic light with angular frequency ω. Subsequently, wave equations for $h_y(x,z)$ and $e_y(x,z)$ are derived:

$$\left(\partial_x^2 + \partial_z^2 + \frac{n(x)^2}{\lambda^2}\right)\Psi(x,z) = 0, \tag{2}$$

where Ψ is h_y and e_y, λ is $\frac{\lambda}{2\pi}$. For the TE mode, we use the boundary condition that $\Psi(x,y)$ and $\partial_x\Psi(x,y)$ are continuous at $|x| = d/2$ and $d/2 + w$, where $n(x)$ discontinuously change. For the TM mode, r.h.s of Eq. (2) becomes $2\partial_x \log[n(x)]\partial_x\Psi(x,z)$. The boundary condition becomes that $\Psi(x,z)$ and $\frac{1}{n^2}\partial_x\Psi(x,z)$ are continuous at $|x| = d/2$ and $d/2 + w$. As we are interested in the TE mode, Ψ means e_y in the following. The other components of electric and magnetic fields are derived from Eq. (2) [3].

Equation (2) is usually solved by separating variables as:

$$\Psi(x,z) = \psi(x)\phi(z), \tag{3}$$

and is written as:

$$\partial_z^2\phi(z) = e\phi(z), \tag{4}$$

$$\left(-\partial_x^2 - \frac{n(x)^2}{\lambda^2}\right)\psi(x) = e\psi(x), \tag{5}$$

where e is a constant number. From Eq. (4), it is obvious that e cannot be positive if the region of z is $-\infty < z < \infty$, because positive e makes $\phi(z)$ diverge in $z \to \infty$ or $z \to -\infty$. For any negative e, there exists positive β such that

$$e = -\beta^2, \tag{6}$$

where β is the propagation constant, and the solution of Eq. (4) represents propagation in positive or negative z-direction with propagation constant $\beta = \sqrt{-e}$.

The problem in solving Eq. (5) is essentially the same as that in solving a one-dimensional Schrödinger equation [10], [11]. The problem to solve Eq. (5) is known as eigenvalue and eigenfunction problem, where e is the eigenvalue and ψ is the eigenfunction for the operator:

$$-\partial_x^2 - \frac{n^2(x)}{\lambda^2}. \tag{7}$$

The eigenfunction is referred to as eigenmode in the following. The solution of Eq. (5) has the following feature: nontrivial solutions of Eq. (5) exist for discrete value of e when e is in the range of $-\frac{n_1^2}{\lambda^2} < e < -\frac{n_2^2}{\lambda^2}$, and for continuous value of e when $-\frac{n_2^2}{\lambda^2} < e$.

In the following section, we solve Eq. (5) with second-order perturbation from a gapless system with suitable approximated integration to calculate the propagation constants for even and odd supermodes. In Sect. 4, we apply our result to one specific model in the existing works [5]–[7] in which propagation constants are calculated using numerical simulations. The final section is devoted to summary and discussion.

3. Perturbative Solution

To solve Eq. (5), we decomposed square of index distribution $n^2(x)$ into square of index distribution at $d = 0$ ($n_0^2(x)$) and the difference between $n^2(x)$ and $n_0^2(x)$ ($n_p^2(x)$) as:

$$n^2(x) = n_0^2(x) + n_p^2(x), \tag{8}$$

where

$$n_0^2(x) = \begin{cases} n_1^2, & |x| < w, \\ n_2^2, & w < |x|, \end{cases} \tag{9}$$

and

$$n_p^2(x) = \begin{cases} n_1^2 - n_2^2, & \left||x| - w - \frac{d}{4}\right| < \frac{d}{4}, \\ -(n_1^2 - n_2^2), & |x| < \frac{d}{2}, \\ 0, & \text{otherwise.} \end{cases} \tag{10}$$

Figure 2 shows the distribution of $n_0^2(x)$ (solid line) and $n_p^2(x)$ (dotted line) on a z = const. line. The squared index distribution of n_0^2 shows that one core is laid on $-w < x < w$. Instead of directly solving Eq. (5), we used the complete set of solution for:

$$\left(-\partial_x^2 - \frac{n_0(x)^2}{\lambda^2}\right)v(x) = ev(x), \tag{11}$$

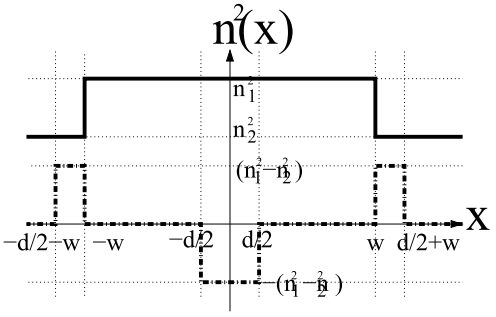

Fig. 2 Decomposition of squared index distributions. Solid line represents $n_0^2(x)$ and dotted line represents $n_p^2(x)$.

to solve Eq. (5), perturbatively. All independent solutions for Eq. (11) are:

$$V_0^s(x)=\begin{cases} v_0^s\cos(\frac{2P_s x}{w}), & |x|<w,\\ v_0^s\cos(2P_s)e^{-\frac{2Q_s(|x|-w)}{w}}, & w<|x|,\end{cases} \tag{12}$$

$$V_0^a(x)=\begin{cases} v_0^a\sin(\frac{2P_a x}{w}), & |x|<w,\\ v_0^a\mathrm{sign}(x)\sin(2P_a)e^{-\frac{2Q_a(|x|-w)}{w}}, & w<|x|,\end{cases} \tag{13}$$

$$V_e^s(x)=\begin{cases} v_e^s\cos(\frac{2P_e x}{w}), & |x|<w,\\ v_e^s\{\cos(2P_e)\cos(\frac{2Q_e(|x|-w)}{w}) & \\ \quad -\frac{P_e}{Q_e}\sin(2P_e)\sin(\frac{2Q_e(|x|-w)}{w})\}, & w<|x|,\end{cases} \tag{14}$$

$$V_e^a(x)=\begin{cases} v_e^a\sin(\frac{2P_e x}{w}), & |x|<w,\\ v_e^a\mathrm{sign}(x)\{\sin(2P_e)\cos(\frac{2Q_e(|x|-w)}{w}) & \\ \quad +\frac{P_e}{Q_e}\cos(2P_e)\sin(\frac{2Q_e(|x|-w)}{w})\}, & w<|x|,\end{cases} \tag{15}$$

where

$$P_s=\frac{\sqrt{n_1^2+e_s}d}{2\lambda},\qquad Q_s=\frac{\sqrt{-(n_2^2+e_s)}d}{2\lambda}, \tag{16}$$

$$P_a=\frac{\sqrt{n_1^2+e_a}d}{2\lambda},\qquad Q_a=\frac{\sqrt{-(n_2^2+e_a)}d}{2\lambda}, \tag{17}$$

$$P_e=\frac{\sqrt{n_1^2+ed}}{2\lambda},\qquad Q_e=\frac{\sqrt{n_2^2+ed}}{2\lambda}. \tag{18}$$

It must be noted that e_s (or the pair of P_s and Q_s) in Eq. (16) and e_a (or the pair of P_a and Q_a) in Eq. (17) satisfies:

$$Q_s\cos(2P_s)=P_s\sin(2P_s), \tag{19}$$

$$P_s^2+Q_s^2=V^2, \tag{20}$$

$$Q_a\sin(2P_a)=-P_a\cos(2P_a), \tag{21}$$

$$P_a^2+Q_a^2=V^2, \tag{22}$$

where

$$V=\frac{\sqrt{n_1^2-n_2^2}d}{2\lambda}, \tag{23}$$

and e in Eq. (18) is a continuous parameter in the region $-n_2^2<e<0$.

V_0^s and V_0^a represent the symmetric and anti-symmetric propagation mode, respectively, and V_e^s and V_e^a represent the symmetric and anti-symmetric radiation modes with eigenvalue e in Eq. (11), respectively.

Here, let us define inner product of fields $\langle f|g\rangle$ as:

$$\langle f|g\rangle=\frac{1}{w}\int_{-\infty}^{\infty}dx f(x)g(x). \tag{24}$$

Then, v_0^s, v_0^a, v_e^s, and v_e^a are defined so that V_0, V_e^s, and V_e^a are normalized to:

$$\langle V_0^p|V_0^p\rangle=\delta^{pq}, \tag{25}$$

$$\langle V_e^p|V_f^q\rangle=\delta^{pq}\delta(e-f), \tag{26}$$

$$\langle V_0^p|V_e^q\rangle=0, \tag{27}$$

where $p,q\in\{s,a\}$, δ^{pq} is the Kronecker delta, and $\delta(e-f)$ is the Dirac delta function. The coefficients in Eqs. (12)–(15) are derived as follows:

$$v_0^s=\sqrt{\frac{2Q_s}{2Q_s+1}}, \tag{28}$$

$$v_0^a=\sqrt{\frac{2Q_a}{2Q_a+1}}, \tag{29}$$

$$v_e^s=\sqrt{\frac{V^2Q_e}{\pi(n_1^2-n_2^2)(Q_e^2\cos^2(2P_e)+P_e^2\sin(2P_e))}}, \tag{30}$$

$$v_e^a=\sqrt{\frac{V^2Q_e}{\pi(n_1^2-n_2^2)(Q_e^2\sin^2(2P_e)+P_e^2\cos^2(2P_e))}}. \tag{31}$$

In the second-order perturbation, the solution for Eq. (5) is determined using Eq. (11) and its orthonormal solution in Eqs. (12)–(15), which are the equation and the solution for the gap-less system. Equation (5) is connected with Eq. (11) using perturbation parameter ϵ as:

$$\begin{aligned}&\left\{\left(-\partial_x^2-\frac{n_0(x)^2}{\lambda^2}\right)-\varepsilon\frac{n_p(x)^2}{\lambda^2}\right\}(V_0(x)+\varepsilon\Delta V^{(1)}(x)+\varepsilon^2\Delta V^{(2)}(x))\\ &=\frac{e_0+\varepsilon\Delta e^{(1)}+\varepsilon^2\Delta e^{(2)}}{\lambda^2}(V_0(x)+\varepsilon\Delta V(x)^{(1)}+\varepsilon^2\Delta V(x)^2),\end{aligned} \tag{32}$$

where $\psi(x)$ and e in Eq. (5) are perturbatively expanded in series of ε and the solution is determined by equating the coefficients of equal power of ε in both sides of Eq. (32) up to ε^2.

The results of Δe_s^1, Δe_s^2, Δe_a^1, and Δe_a^2 are [10], [11]:

$$\Delta e_s^{(1)}=-\left\langle V_0^s\left|\frac{n_p^2}{\lambda^2}\right|V_0^s\right\rangle,\qquad \Delta e_a^{(1)}=-\left\langle V_0^a\left|\frac{n_p^2}{\lambda^2}\right|V_0^a\right\rangle, \tag{33}$$

$$\Delta e_s^{(2)}=\sum_{e\neq e_s}\frac{|\langle V_0^s|\frac{n_p^2}{\lambda^2}|V_e^s\rangle|^2}{e-e_s},\qquad \Delta e_a^{(2)}=\sum_{e\neq e_a}\frac{|\langle V_0^a|\frac{n_p^2}{\lambda^2}|V_e^a\rangle|^2}{e-e_a}. \tag{34}$$

In our case, Eq. (34) is symbolic because e, which is an eigenvalue of Schrödinger equation (5), is a continuous parameter. Therefore, we must rewrite Eq. (34) for continuous parameter:

$$\Delta e_s^{(2)} = \lambda^2 \int_{e_{\min}}^{e_{\max}} de\rho(e) \frac{|\langle V_0^s|\frac{n_p^2}{\lambda^2}|V_e^s\rangle|^2}{e - e_s}, \tag{35}$$

$$\Delta e_a^{(2)} = \lambda^2 \int_{e_{\min}}^{e_{\max}} de\rho(e) \frac{|\langle V_0^a|\frac{n_p^2}{\lambda^2}|V_e^a\rangle|^2}{e - e_a}, \tag{36}$$

where $\rho(e)$ represents mode density, and the coefficient λ^2 is introduced to keep the dimension of $\Delta e^{(2)}$ consistent with e_0 and $\Delta e^{(1)}$.

It can be noted that for any symmetric field $f(x)$, $\langle f|\frac{n_p^2}{\lambda^2}|V_0^s\rangle$ is:

$$\begin{aligned}
&\left\langle f|\frac{n_p^2}{\lambda^2}|V_0^s\right\rangle \\
&= -\frac{2(n_1^2 - n_2^2)}{\lambda^2 w}\left(\int_0^{\frac{d}{2}} dx f(x)V_0^s(x) - \int_w^{w+\frac{d}{2}} dx f(x)V_0^s(x)\right), \qquad (37)\\
&= -\frac{(n_1^2 - n_2^2)}{\lambda^2}\frac{d}{w}\left(f(0)V_0^s(0) + \frac{d}{dx}\left(f\left(\frac{d}{2}\right)V_0^s\left(\frac{d}{2}\right)\right)\frac{d}{4w}\right.\\
&\left. -f(w)V_0^s(w) - \frac{d}{dx}\left(f\left(w+\frac{d}{2}\right)V_0^s\left(w+\frac{d}{2}\right)\right)\frac{d}{4w}\right) + o\left(\frac{w}{d}\right)^3, \qquad (38)
\end{aligned}$$

where the trapezoidal method is used to deform from Eq. (37) to Eq. (38). Similarly, for any anti-symmetric field $g(x)$, $\langle g|\frac{n_p^2}{\lambda^2}|V_0^a\rangle$ is also calculated. By using Eqs. (12)–(15), we can obtain the the second-order Taylor expansion of $\frac{d}{w}$ for $\Delta e_s^{(1)}, \Delta e_a^{(1)}, \Delta e_s^{(2)}$, and $\Delta e_a^{(2)}$ as:

$$\Delta e_s^{(1)} = \frac{2Q_s(n_1^2 - n_2^2)}{(2Q_s+1)\lambda^2}\frac{w}{d}\left(\sin^2(2P_s) + \cos^2(2P_s)\frac{d}{w}\right), \tag{39}$$

$$\Delta e_a^{(1)} = \frac{2Q_a(n_1^2 - n_2^2)}{(2Q_a+1)\lambda^2}\frac{w}{d}\left(-\sin^2(2P_a) + \sin^2(2P_a)\frac{d}{w}\right), \tag{40}$$

$$\Delta e_s^{(2)} = -\frac{2Q_s(n_1^2 - n_2^2)V^2}{(2Q_s+1)\pi\lambda^2}\left(\frac{d}{w}\right)^2 I_s, \tag{41}$$

$$\Delta e_a^{(2)} = -\frac{2Q_a(n_1^2 - n_2^2)V^2}{(2Q_a+1)\pi\lambda^2}\left(\frac{d}{w}\right)^2 I_a, \tag{42}$$

where

$$I_s = \int_{-n_2^2}^{0} de \frac{\rho_s(e)Q_e(1 - \cos(2P_s)\cos(2P_e))^2}{(e - e_s)(Q_e^2\cos^2(2P_e) + P_e^2\sin^2(2P_e))}, \tag{43}$$

$$I_a = \int_{-n_2^2}^{0} de \frac{\rho_a(e)Q_e\sin^2(2P_a)\sin^2(2P_e)}{(e - e_a)(Q_e^2\sin^2(2P_e) + P_e^2\cos^2(2P_e))}, \tag{44}$$

where $\rho_s(e)$ and $\rho_a(e)$ are mode densities for the symmetric and anti-symmetric radiation modes, respectively, and where P_e and Q_e are defined in Eq. (18).

It should be noted that Eqs. (33), (34) suggest that the order of perturbation coincides with the order of power of $n_1^2 - n_2^2$ because the order of perturbation coincides with the order of $n_p^2(x)$, which is proportional to $n_1^2 - n_2^2$. Although it is shown in Eqs. (41), (42), $\Delta e_s^{(2)}$ and $\Delta e_a^{(2)}$ include $n_1^2 - n_2^2$, they also include $V^{2\dagger}$, which is proportional to $n_1^2 - n_2^2$, thus they are proportional to $(n_1^2 - n_2^2)^2$. It means that the perturbative analysis is valid if $n_1^2 - n_2^2 \ll 1$.

4. Comparison with Existing Works

In [5]–[7], propagation constants for the symmetric and anti-symmetric supermodes in the TE mode for two parallel waveguide arrays with parameters of $n_1 = 2.2$, $n_2 = 2.19$, $w = 2.0\,\mu$m, and $d = 1.95\,\mu$m have been calculated. In these works, almost the same propagation constants had been obtained as follows:

$$\beta_s = \begin{cases} 13.01634 & \text{result in [5], [6],} \\ 13.0162 & \text{result in [7],} \end{cases} \tag{45}$$

$$\beta_a = \begin{cases} 13.01096 & \text{result in [5], [6],} \\ 13.0110 & \text{result in [7].} \end{cases} \tag{46}$$

It must be noted that we must calculate integral in Eqs. (41), (42) to calculate the propagation constants in second-order perturbation. However, as $\rho(e)$ is unclear, we had calculated these integrals with $\rho(e) = 1.0$ and 1.5. We should note that the maximum value of the integral domain is zero because we want to add all the effects of radiation modes. However, for the equivalent quantum mechanical system, the maximum value should be infinity.

Figure 3 shows the curves of $\beta(\frac{d}{w})$ on $0 \le \frac{d}{w} \le 1$. It should be noted that the propagation constants in Fig. 3 and Δe discussed in the previous section have relationship in Eq. (6) and

$$\beta\left(\frac{d}{w}\right) = \sqrt{\beta_0^2 - \Delta e^{(1)} - \Delta e^{(2)}} + O\left(\frac{d}{w}\right)^3 \tag{47}$$

$$= \beta_0 - \frac{\Delta e^{(1)} + \Delta e^{(2)}}{2\beta_0} - \frac{(\Delta e^{(1)})^2}{8\beta_0^3} + O\left(\frac{d}{w}\right)^3, \tag{48}$$

where β_0 is a propagation constant at $\frac{d}{w} = 0$. Figure 3(a) shows the result of first-order perturbation. The red and blue dotted lines show $\frac{d}{w}$ corrections of propagation constants for the symmetric and anti-symmetric modes, respectively, and the red and blue solid lines show $(\frac{d}{w})^2$ correction of these.

Equations (33) and (48) without $\Delta e^{(2)}$ explain the behavior of curves shown in Fig. 3(a), presenting the negative coefficients of $\frac{d}{w}$ in β_s and $(\frac{d}{w})^2$ in both propagation constants, and positive coefficient of $\frac{d}{w}$ in β_a. As shown in Eqs. (12) and (13), $e_s^{(1)}$ and $e_a^{(1)}$ have terms proportional to $(\frac{d}{w})^2$. Moreover, the third term of Eq. (48) also have coefficients of $(\frac{d}{w})^2$. Because of these terms, the solid lines are not straight.

†When perturbation calculation includes radiation mode, V^2 arises instead of $n_1^2 - n_2^2$ because of coefficients of normalized radiation mode wave functions in Eqs. (30), (31).

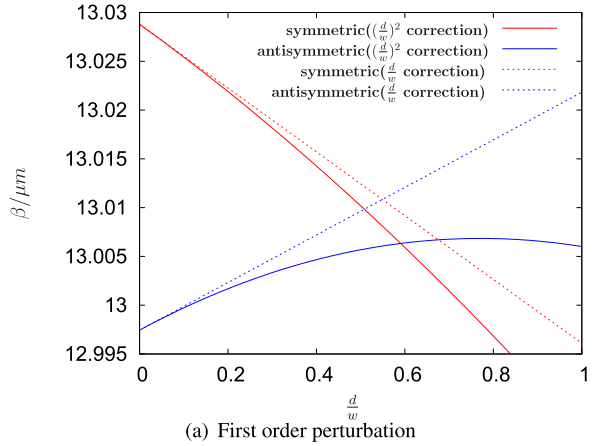

(a) First order perturbation

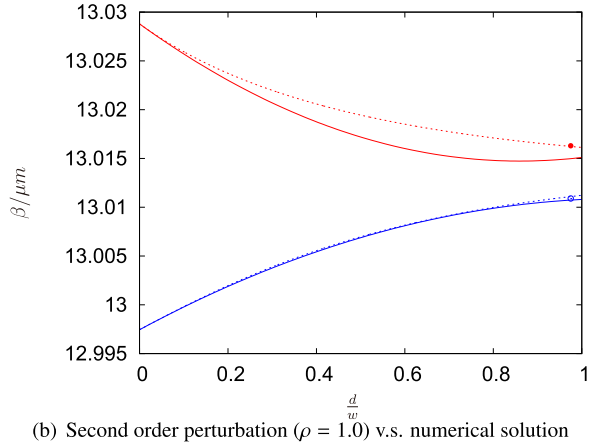

(b) Second order perturbation ($\rho = 1.0$) v.s. numerical solution

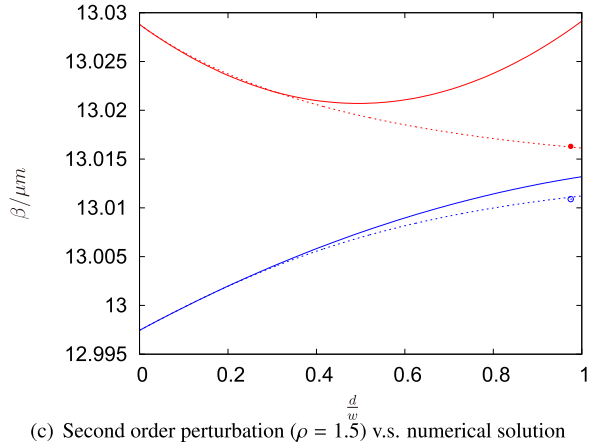

(c) Second order perturbation ($\rho = 1.5$) v.s. numerical solution

Fig. 3 Analytic and numerical results.

Figures 3(b) and 3(c) show the behavior of propagation constants. The red and blue solid lines show the result of second-order perturbative correction for the symmetric and anti-symmetric modes, respectively, when $\rho = 1.0$ in Fig. 3(b), and when $\rho = 1.5$ in Fig. 3(c). In these figures, the red and blue dotted lines show the accurate solutions of the symmetric and anti-symmetric modes, respectively, obtained by finding the roots of the transcendental equation, through field matching at the dielectric interfaces. Circles at $\frac{d}{w} = 0.975$ are the results of previous works [5]–[7]. Figures 3(b) and 3(c) shows that the second order perturbation improves the behavior of both coupling constants. In Fig. 3(b), the curves of second order perturbation and numeric solutions for the anti-symmetric mode have a substantial overlap with each other. However, the curves for the symmetric mode have an overlap only when $\frac{d}{w}$ is less than about 0.1. In Fig. 3(c), the curves for both modes have an overlap when $\frac{d}{w}$ is less than about 0.3. Comparing Figs. 3(b) and 3(c), the second order perturbation for the symmetric mode is more sensitive to change of ρ than that for the anti-symmetric mode.

In any figures in Fig. 3, the coefficient of $\frac{d}{w}$ for the perturbation result of the symmetric mode is -0.0327 and one for that of the anti-symmetric mode is 0.0244. On the other hand, the slopes of accurate solutions at $\frac{d}{w} = 0$ in Figs. 3(b) and 3(c) for the symmetric and anti-symmetric modes are -0.0327 and 0.0244, which are the same as the perturbation results. This coincidence supports validity of first terms for Eqs. (39), (40), and also supports validity of using trapezoidal method in Eq. (37)[†].

5. Conclusion and Discussion

For the symmetric supermode, the propagation constant decreases according to increasing $\frac{d}{w}$ from $\frac{d}{w} = 0$, and the curve becomes convex downward. For the anti-symmetric supermode, the propagation constant increases according to increasing $\frac{d}{w}$ from $\frac{d}{w} = 0$, and the curve becomes convex upward. We have shown that second-order perturbation with the trapezoidal method gives at least qualitative behavior shown earlier, despite using an assumption that the mode density $\rho(e) = 1.0$ and $\rho(e) = 1.5$. In Fig. 3(b), it seems that the perturbation result of the anti-symmetric mode is in good agreement with the accurate solution, although the perturbation result of the symmetric mode does not agree with the accurate solution.

However, as shown in Fig. 4, the difference between the perturbation and accurate solutions for the anti-symmetric mode at $\rho = 1.5$ is smaller than that at $\rho = 1.0$ in the region of $\frac{d}{w} \lesssim 0.3$. In general, the smaller the expansion parameter becomes, the more accurate becomes an approximation based on the Taylor expansion. Therefore, the agreement of the perturbation and accurate results for the anti-symmetric mode in Fig. 3(b) is coincidental.

It should be noted that Eq. (34), the second order perturbation, is based on the completeness relationship for the gap-less system:

$$\sum_{i=a,s}\left[V_0^i(x)V_0^i(y) + \sum_e V_e^i(x)V_e^i(y)\right] = \delta(x-y), \qquad (49)$$

where $\delta(x)$ is Dirac delta function and where $\sum_e$ is symbolic because e is continuous parameter. Equation (49) means

[†]We have analytically shown in Ref. [12] that the coefficient of $\frac{d}{w}$ for the perturbation results of e in the symmetric mode coincides with the slope of the accurate solution at $\frac{d}{w} = 0$.

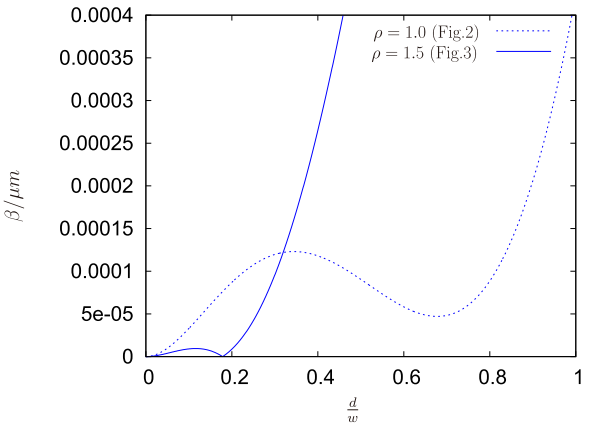

Fig. 4 The absolute value of the difference between the second order perturbation and accurate solutions for the anti-symmetric mode at $\rho = 1.0$ and $\rho = 1.5$.

that any field can be expanded by propagation and radiation modes and teaches expansion procedure. Practically, the sum of e in Eq. (49) is calculated by integral over a suitable range of e, which distinguishes radiation mode from each other. Notice that we can use other parameter, for example $\beta = \sqrt{-e}$. Because of such an ambiguity of parameter selection, when we rewrite the sum over e to integral over e, we must know the mode density that satisfies:

$$\sum_e V_e^i(x)V_e^i(y) = \int_{e_{min}}^{e_{max}} de\rho(e)V_e^i(x)V_e^i(y). \tag{50}$$

However, the exact form of the mode density is unknown, we can only show the possibility that the second order perturbation can improve the behavior for the propagation constants for supermodes. We think that quantitative behavior for the propagation constants of supermodes could be explained by using the exact mode density.

Here, let us comment on the first sentence of Sect. 2, "two symmetric slab waveguides are configured in parallel." When two waveguides are sufficiently separated, this statement is valid because theory such as coupling mode theory, in which electromagnetic field is expanded by eigenmodes of the respective waveguides, is valid from the viewpoint of perturbation theory. This means that there is no difference between the statement and basis modes of theory. We can understand that the basis modes of theory is given by zeroth order of perturbation [1]–[3]. However, when the gap between two-slab waveguides is small enough, the theoretical analysis based on eigenmodes of respective waveguides becomes invalid. Instead of using such eigenmodes, supermodes, which are eigenmodes of one waveguide having index distribution shown in Fig. 1(b) or Eq. (1), are used to analyze the optical properties. The supermodes are perturbatively determined from eigenmodes of one multimode slab waveguide. Therefore, to match the statement "one multimode slab-like waveguide having index distribution of Eq. (1)" would be preferable match the statement on theoretical analysis.

Acknowledgment

We thank all the members of Tobe Laboratory, Department of Integrated Information Technology, College of Science and Engineering, Aoyama Gakuin University, for their valuable discussions and comments.

References

[1] A. Yariv, "Coupled-mode theory for guided-wave optics," IEEE J. Quant. Electron., vol.QE-9, pp.919–933, 1973.
[2] A. Hardy and W. Streifer, "Coupled Mode Theory of Parallel Waveguides," J. Lightwave Technol., LT-3, pp.1135–1146, 1985.
[3] D. Marcuse, Theory of Dielectric Optical Waveguides, Second ed., Academic Press, New York, 1991.
[4] A. Ghatak and V. Lakshminarayanan, "Propagation characteristics of planar waveguides," in Optical Waveguides from Theory to Applied Technologies, ed. M.L. Calvo, and V. Lakshminarayanan, CRC Press, Boca Roton, 2007.
[5] T. Wongcharoen, B.M.A. Rahman, and K.T.V. Grattan, "Electro-optic directional coupler switch characterization," J. Lightwave Technol., vol.15, pp.377–382, 1997.
[6] P.R. Chaudhuri and S. Roy, "Analysis of arbitrary index profile planer optical waveguides and multilayer nonlinear structures: A simple finite difference algorithm," Opt. Quant. Electron., vol.39, pp.221–237, 2007.
[7] C.C. Huang, C.C. Huang, and J.Y. Yang, "An efficient method for computing optical waveguides with discontinuous refractive index profiles using spectral collocation method with domain decomposition," J. Lightwave Technol., vol.21, pp.2284–2296, 2003.
[8] Y. Suematsu and K. Kishino, "Coupling coefficient in strongly coupled dielectric waveguides," Radio Sci., vol.12, pp.587–592, 1977.
[9] B. Broberg, B.S. Lindgren, M.G. Öberg, and H. Jiang, "A novel Integrated Optics Wavelength Filter in InGaAsP-InP," J. Lightwave Technol., vol.4, pp.196–203, 1986.
[10] L.I. Shiff, Quantum Mechanics, Mc-Graw Hill, Singapore 1969.
[11] W. Greiner, Quantum Mechanics — An Introduction, Springer-Verlag Berlin and Heidelberg GmbH & Co. K, 1989.
[12] N. Kitsunezaki, "Perturbation analysis with approximate integration for propagation mode in two-dimensional two-slab waveguides," IRSN Optics vol.2013, 108704, 2013.

Naofumi Kitsunezaki was born in 1973. He studied in the field of super-string theory, and received Ph.D. from Nagoya University, Nagoya, Japan, in 2001. He is now working in Aoyama Gakuin University as a research associate, and working in the field of optical waveguide analysis.